Investigation of sound radiation by automotive tyres vibrating at low resonant frequencies

Investigation of sound radiation by automotive tyres vibrating at low resonant frequencies

A.C. Wood [1], V.V. Krylov [1], S.J. Walsh [1]
[1] Department of Aeronautical and Automotive Engineering, Loughborough University, Loughborough, Leicestershire, LE11 3TU, UK
e-mail: **V.V.Krylov@lboro.ac.uk**

Abstract
In this work, the experimental study was conducted to identify the resonant frequencies and modal shapes of an automotive tyre. Further work was undertaken to determine the sound radiation characteristics of the tyre excited at these resonant frequencies. The obtained experimental results can be used for better understanding of the structural resonant behaviour of the tyre and of its sound radiation. A simple theoretical model was developed to describe sound radiation by tyre vibration modes. The model uses combinations of acoustic monopoles to represent a tyre vibrating over the first four modes of vibration. A good agreement was achieved between the normalised acoustic pressure plots predicted by the model and those measured in the anechoic chamber.

1 Introduction

Recent studies show that tyre noise accounts for more than 60% of overall vehicle noise when conducting a vehicle drive-by test at speeds around 60 kph. Tyre noise becomes even more important as vehicle speeds increase. Various mechanisms are responsible for noise generated by vehicles tyres [1-3]. They can be separated into two main categories: structure-borne noise associated with tyre vibration [4-12] and aerodynamic noise associated with the air pumping effect and other related mechanisms [13-15].

Radial vibrations of the tyre belt and associated profile elements (tread) are the dominant tyre noise generation mechanism below 1 kHz [5]. The rubber of the tyre and the tread elements is very soft with a low shear modulus and a high poisons ratio in comparison to the road surface. The tyre will therefore deform according to the road roughness and wheel rotation, the leading edge will be deformed as the tyre strikes the road and the trailing edge is excited as the tyre springs away from the road surface. The tread element has a high vertical velocity component just before it contacts with the road surface, this is reduced to zero in a short period of time. It is the large accelerations and load modulation that causes the tyre vibration. The level of vibration varies with the amplitudes and wavelengths of the road profile making the forcing functions for the road generally random. These induced vibrations then spread over the entire tyre carcass/tyre wall causing radiation of air-borne noise, which is to be the primary investigation of this paper.

There are several types of theoretical models describing tyre vibrations: models based on a circular ring on an elastic foundation, models employing a cylindrical shell, or more realistic models using finite element calculations. A circular ring based on an elastic foundation is one of the first models used for describing tyre vibrations. In particular, the ring model used by Kropp [4] gave a good description of the tyre vibration of a smooth tyre up to 400 Hz. It showed that below 250 Hz the tread behaved as a string under tension, and between 250-400 Hz it behaves as a beam. Shell models treat the tyre as a 3-dimensional object. The tyre is viewed as an equivalent thin shell, and the response of the tyre is described using a 3-dimensioal Greens function.

In order to gain a more in depth knowledge into the scope of the vibration /noise model it is necessary to investigate the vibrating regions of the tyre. Kropp's vibration model [4] only includes radial vibration mechanisms and accurately describes tyre vibration up to 400 Hz. He also showed that sidewall vibration

does not significantly contribute to sound radiation. Perisse [8] looked into the relationship further. He found that the tread response dominates the sidewall response particularly above 1000 Hz, where the difference is typically greater than 20 dB. At lower frequencies, between 500-800 Hz, the difference is less significant, as it follows from the research by Iwao et al [16] who attributes the sidewall vibration as a noise generating mechanism in this region. Furthermore, two simple models for estimating tyre noise radiation levels were presented by Cuschieri et al [17]. The first estimates the radiated sound assuming the tyre is a ring in an infinite cylindrical baffle vibrating at a constant amplitude along the axial direction therefore only the radial surface motion has an influence. Secondly, the alternative model is to estimate the radiated acoustic power by considering the tyre as a circular ring of monopole sound sources, with the source strength of the monopoles being equivalent to the tyres response at each angular location. Both models gave an adequate prediction of sound power level output when compared to measured results in an anechoic chamber.

The aim of this paper is to investigate structural vibrations and the associated sound radiation of a tyre for the first few modes of tyre vibration which are in the region of 100-300 Hz as these vibration modes account for the largest percentage of vehicle tyre noise emission in this frequency band. The paper will focus on the vibrational and noise radiation behaviour of a static automotive tyre undergoing radial excitation on its first four fundamental modes of vibration. The paper is split into three main sections.

1. Tyre Vibration Testing – The vibrational characteristics of the tyre are studied to determine the fundamental frequencies of the tyre and then determine the modal response of the tyre when excited at each of these frequencies.
2. Acoustic Experimental Testing – The noise radiation characteristics of the tyre through its horizontal mid plane and radial directions when excited at its fundamental frequencies are measured to allow comparison with and help develop a simple theoretical model to describe the tyres noise radiation patterns.
3. Theoretical Modelling – Using the results gathered from the experimental testing about the vibration amplitudes of the tyre along with the assumption that the modal response of the tyre can be approximated to that of ideal thin walled cylindrical shells, a simple model for the tyre noise radiation patterns is developed. Using appropriate combinations of acoustic monopoles, the developed theoretical model is used to generate results that allow direct comparison with the acoustic testing.

Due to the scope of this paper that will be investigating only the first few modes of vibration of the tyre it may not be accurate to disregard the sidewalls in the radiation modelling when only investigating up to frequencies circa 400 Hz. In the testing section sidewall and tread vibration will be investigated further with particular respect to the frequency range of concern. If it is determined that there is a good coherence between sidewall and tread vibration and that the radial tread vibration is dominant then using a monopole model has distinct advantages. As a monopole radiates sound equally in all directions the sidewall and tread vibration become encapsulated in the resultant sound pattern as long as the measurements are made at a significant distance (to avoid the near field sound region where the tyre shape sidewall/rim/tread areas will make large pressure differences with respect to small changes in the receiver location) that the tyre can be approximated to a number of monopoles distributed around its circumference.

2 Experimental testing

Two stages of measurements took place:

- Stage 1 - To identify the resonant frequencies of the tyre vibration and the corresponding modal shapes. To compare the modal shapes with those for the idealised thin-walled cylinders.
- Stage 2 - To identify the sound radiation patterns in the horizontal mid-plane generated by the tyre vibrating at its resonant frequencies To compare the results to the radiation patterns given by the simple theoretical model. To identify the near-field acoustic pressure in the vertical plane.

2.1 Tyre vibration measurements

2.1.1 Overview

The tyre, 155/65/R13 (smooth), was excited by a dynamic shaker device and the accelerance at a point close to the excitation was measured, where accelerance is the acceleration of the measured point per unit force input. The force was applied via a thin threaded shaft to the base of the tyre (Figure 1). A force transducer (Bruel & Kjaer) was attached between the tyre and end of the shaker to measure the force input to the tyre.

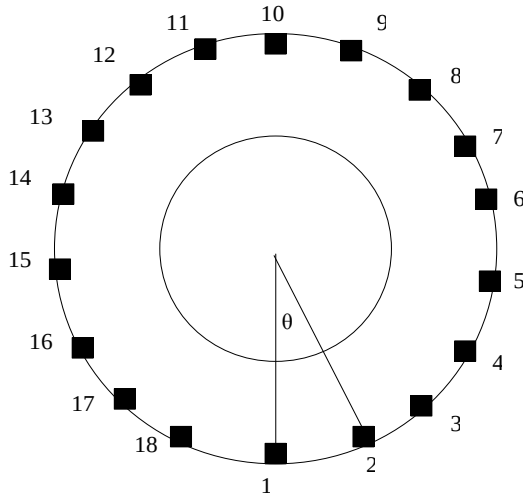

(a)

(b)

Figure 1: Shaker and accelerometer position on a tyre: (a) Accelerometer positions 1-18, angle θ=20 deg between points, and excitation is at position 1; (b) Shaker and accelerometer set up.

The frequency of the excitation to determine the modal frequencies was initially over a broad range of 0-2 kHz, which was narrowed as the first few resonant frequencies become clear. RT_Photon software was used to generate the input signal to the dynamic exciter (a white noise signal) and was also used as the FFT (Fast Fourier Transform) analyser. The analyser averaged the frequency response measurements 30 times for accuracy and to remove cyclic variation. The tyre was mounted on a relatively heavy steel rig which can be seen in Figure 1. Once the key frequencies have been identified the accelerometer was positioned circumferentially at intervals of 20 degrees around the tyre (see Figure 1(a)). The tyre was then excited over the narrower range of 0-400 Hz to reflect the frequencies of modal response. The relationship of the frequency response of one location to another was built up over the whole tyre leading to a set of frequency response functions (FRF's). Each measuring location was subjected to the same white noise input signal. Particular care was given to monitoring tyre inflation pressure which can alter the natural frequencies of each mode and the vibration levels in the tyre.

2.1.2 Tread, sidewall and rim vibrations

The accelerometer was mounted at position 1 (Figure 1(a,b)) on the tread, sidewall and rim and the accelerance was measured for a white noise input by the radially mounted shaker. The tyre was set to its

rated inflation pressure of 30 psi. The results are shown in Figure 2. It can be seen from Figure 2 that the vibration levels of the rim are very small in comparison to the tyre and sidewall, except for the first resonant frequency where there is a correlation between the vibration amplitude of the rim, sidewall and tread. From this it can be concluded that vibrations of the construction do not have an impact on the measurements except possibly for the first natural frequency. Secondly, the sidewall and tread vibrations in the lower frequency region 100-300 Hz show a strong correlation as expected. Although the level of vibration is lower in the sidewalls, it is still significant. Between 300-600 Hz the sidewall accelerance dominates that of the tread, which implies that it is the key vibration and radiation mechanism at these frequencies, which agrees with Iwao et al [16]. This is due to the cross sectional bending modes which start to appear in this frequency range. Above 500-600Hz the dominant vibration mechanism clearly becomes the tread.

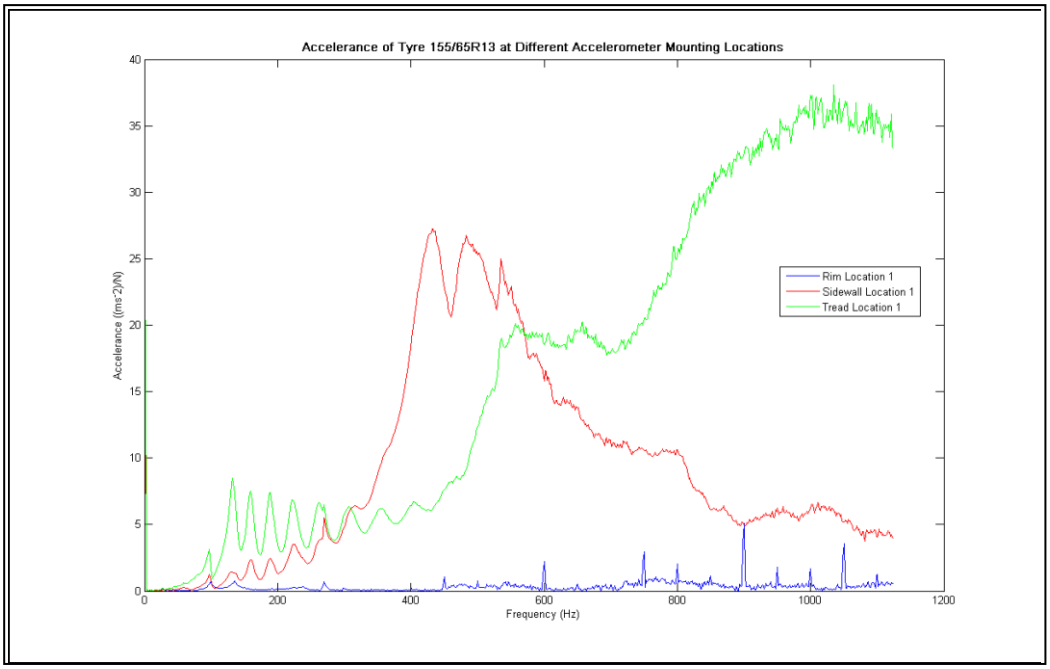

Figure 2: Measured tyre accelerance at a rim, a tread and a sidewall.

It is possible to see patterns in Figure 2 which show the different wave types and responses of the tyre. In the very low frequency range, 25-90 Hz, the tyre behaves like a spring with a stiffness constant and loss factor. In the frequency range 90-300 Hz the response is governed by the resonances of the tyre. The tyre response is that of an infinite beam with tension, and bending waves being the predominant wave type. It can be seen that for frequencies above 400 Hz that the vibration level greatly increases, this is the cut on frequency for longitudinal waves where the tyre no longer responds as a beam but as a plate. At 1 kHz there is a significant peak in tread vibration levels. It is possible therefore that this tread vibration is a major contributory factor in the multi-coincidence peak that can be seen in the frequency spectra for tyre/road noise.

2.1.3 Inflation pressure effect on tyre resonances

In order to determine the importance of the monitoring of inflation pressure during testing a study was conducted to see the effect of inflation pressure on tyre resonance. The experimental set up is the same as in section 2.1.1, and the frequency response of the tyre under a white noise input signal (0-1 kHz) is analysed. The electrodynamic exciter and accelerometer were not moved during this test so that the only variable was the inflation pressure which was varied from 5psi (34 kPa) to the rated pressure of 30 psi (207 kPa).

Figure 3 shows the measured results of natural frequency for the first 6 modes in the radial direction. When inflation pressure is increased the natural frequency for any particular mode is transferred to a higher frequency, the relationship is linear. The linear relationship confirms a typical mass/spring system response with an increase in inflation pressure resulting in an increase in stiffness of the sidewalls, hence higher resonant frequency.

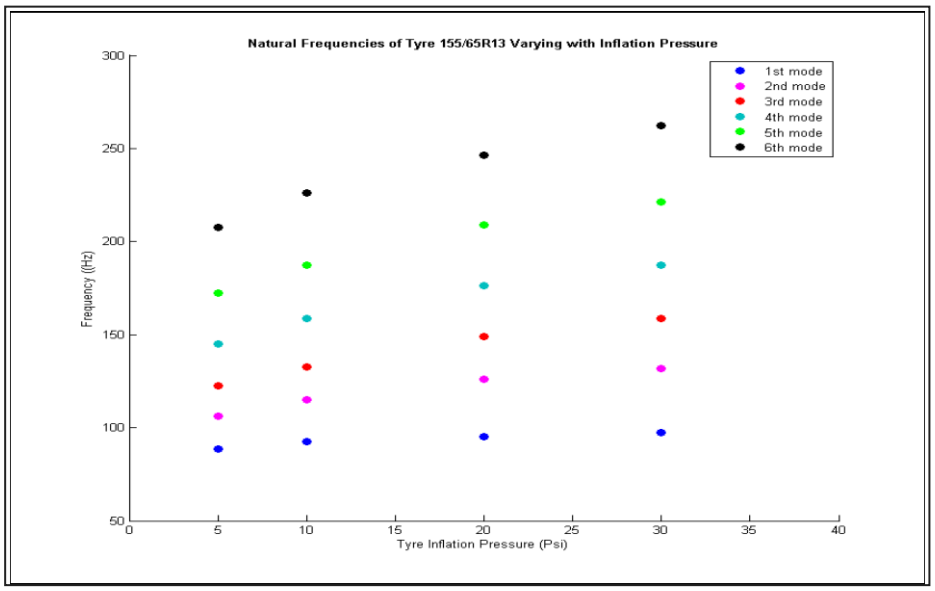

Figure 3: Resonant frequencies of the first six modes under varying inflation pressure.

2.1.4 Resonant frequencies and mode shapes

The first 8 natural frequencies measured on the tyre are indicated in Table 1. The mode shapes were determined using the measured values of accelerance for each natural frequency at each of the 18 circumferential locations around the tyre. The normalised mode shapes of the first 4 radial modes of the tyre can be seen in Figure 4(a-d). Each mode shape corresponds to the theoretical mode shape response. The resolution of the measurement locations, only measuring every 20 degrees, is acceptable for measuring the first few mode shapes. However, due to the complexity of the higher order mode shapes, it is not possible to accurately display their associated radial mode shape. For the purpose of this study only the first four modes have been examined. The asymmetry of the results indicate that there could be errors in the positioning of the accelerometer accurately over its 20 degree interval. Also the actual symmetry of the tyre carcass mounted on the rig could have inherent asymmetry.

Mode Number	Frequency
n=1	97.5
n=2	132.5
n=3	158.8
n=4	188.8
n=5	222.5
n=6	262.5
n=7	306.3
n=8	353.8

Table 1: First eight resonant frequencies of the tyre.

Note that there is a strong correlation in the observed first four vibration modes of the tyre and the theoretically predicted vibration modes of circular cylindrical shells [18]. In the case of cylindrical shells, the n=0 mode is called the 'breathing' mode in which the radius of the cylinder expands and contracts acting as a single monopole source. In the n=1 mode the cylinder oscillates back and forth acting as a dipole pair. The n=2 mode acts as a quadrupole, etc. It seems to be plausible to model sound radiation by different modes of vibration of a tyre as radiation by combinations of equivalent monopole sound sources with their source strengths proportional to those of the relative vibration amplitudes seen in Figures 4(a-d).

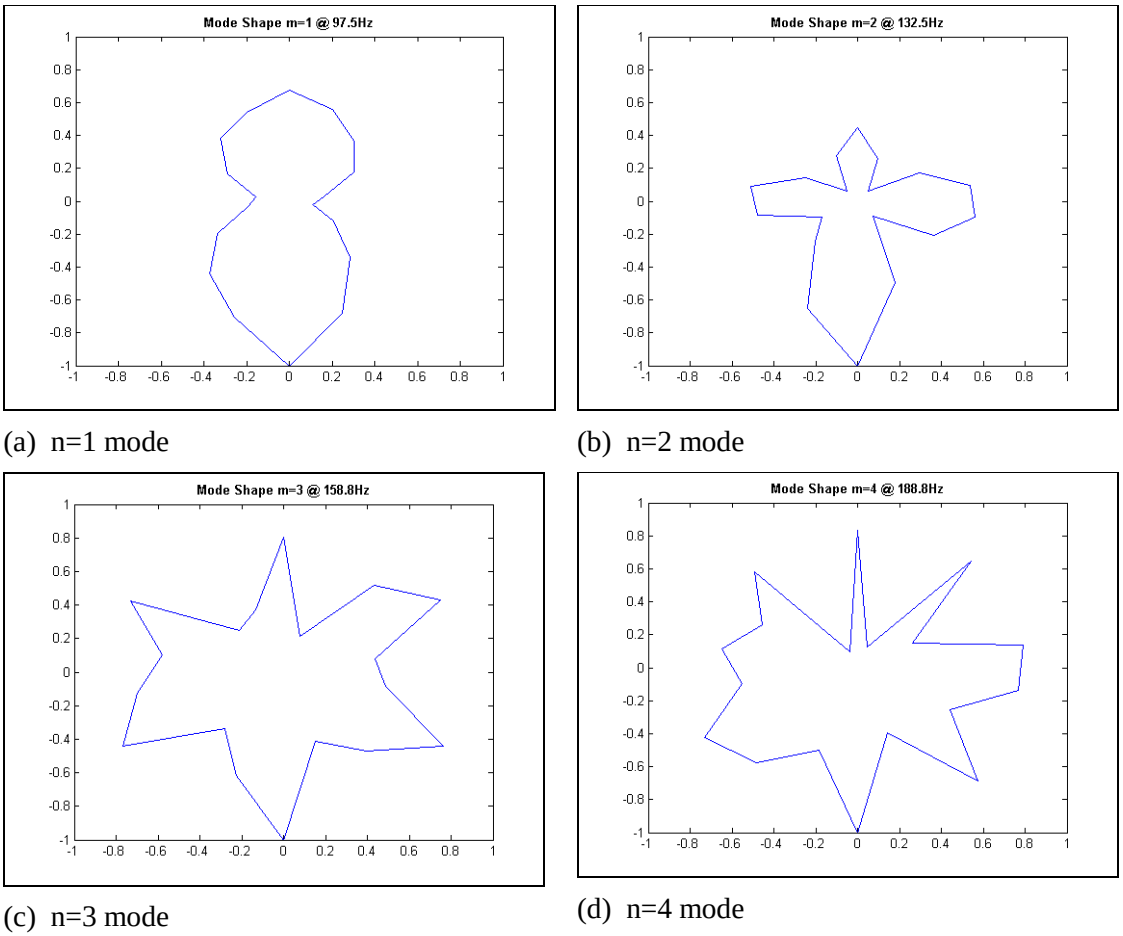

(a) n=1 mode (b) n=2 mode

(c) n=3 mode (d) n=4 mode

Figure 4: Measured mode shapes for the first four modes of the tyre.

2.2 Sound radiation measurements

2.2.1 Overview

The second stage of testing included measurements of the sound radiation characteristics of the tyre vibrating over its first four modes of vibration. All the measurements were conducted in an anechoic chamber. The sound radiation characteristics of the tyre were measured in two planes at the first four resonant frequencies of tyre vibration.

1. A horizontal sound radiation pattern measured on the horizontal mid plane of the tyre at a distance large enough to avoid the effects of near field sound.

2. A vertical (circumferential) sound radiation field around the tyre. Due to accessibility restrictions this would include only near field sound radiation. The measurements would be conducted to relate them directly to the tyre vibration patterns that were determined in the stage 1 testing.

2.2.2 Horizontal far field measurements of radiated sound

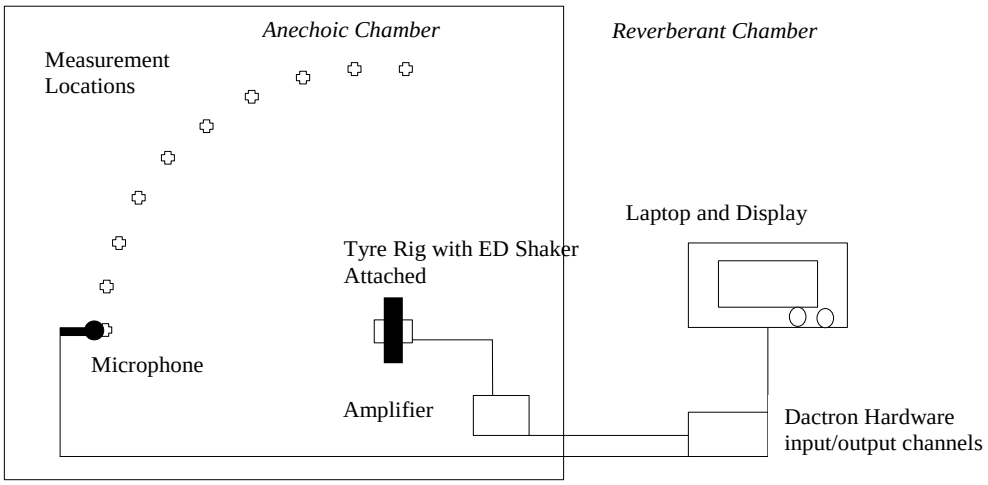

Figure 5: Top view of the experimental set up for measurements in the horizontal mid plane.

The experimental setup for measuring the radiation pattern in the horizontal mid plane can be seen in Figure 5. As previously, RT_Photon software was used to generate the input signal at the correct frequency for each mode to the electrodynamic exciter. For these tests the tyre was excited sinusoidally at each individual frequency and measurements taken. The electrodynamic exciter setup was kept the same as in the case of tyre vibration measurements. A 90 degree arc was then drawn beginning at point 1 perpendicular to the tyre centre.

The microphone position in Figure 5 was moving in 5 degree intervals, ending at point 19 perpendicular to the tyre tread. The microphone was a Bruel and Kjaer type-4133. Care was taken to ensure the microphone is normal to the tyre centre point with each measurement. In addition to this, care was taken to ensure that the anechoic chamber is emptied of all other objects that could cause sound reflection. The microphone was kept at 2.5 m from the tyre, which gave almost 3 whole wavelengths from the source vibrating at its lowest frequency. Therefore, this was an acceptable distance for far field measurements, and repeatable results were being achieved in this circumstance.

2.2.3 Vertical near field measurements of radiated sound

For this experiment the tyre was excited at each natural frequency, but sound pressure measurements were taken in intervals around the circumference of the tyre. The results were taken with the microphone being positioned at a distance of 100 mm from the surface of the tyre. Due to restriction in the location of the apparatus only the top of the tyre could be measured. The results were then mirrored over the circumference of the tyre. This affected the validity of the results for the lower half of the tyre where asymmetry in the magnitude could be expected.

3 Theoretical modelling of tyre sound radiation using combinations of acoustic monopoles

The vibration testing results as seen in Figure 4(a-d) clearly indicate that the tyre under radial excitation over its first four modes of vibration behaves in a way similar to that seen in equivalent thin walled cylindrical shells or rings. In order to model the sound radiation patterns produced by the tyre when vibrating on these first four modes the tyre in this work was approximated by limited numbers of acoustic monopoles positioned over its circumference. The model was then used to compare firstly with the radiation pattern about the horizontal mid plane and secondly with the radial near field patterns. The minimum number of monopoles is dependent on the mode of vibration. For the n=1 mode describing a simple oscillatory motion the tyre is approximated to a system of two monopoles acting in opposite phases. The n=2 mode is a four monopole system, the n=3 mode is a six monopole system, and the n=4 mode is an eight monopole system.

3.1 Calculation of distances from each monopole source to observation point

The first stage in the model was to calculate the distances for each of the source monopoles to the receiver (microphone) for each position either along the horizontal mid plane or the vertical radial plane. The second stage involved calculation of the acoustic pressure radiated by each of the monopoles and taking a superposition of these pressures at the point of observation. Each monopole was scaled to relate its volume velocity (strength) to the measured vibration amplitudes.

For example, for the n=2 mode the tyre is modelled as a four monopole sources with opposing monopoles having the same phase (see Figure 6).

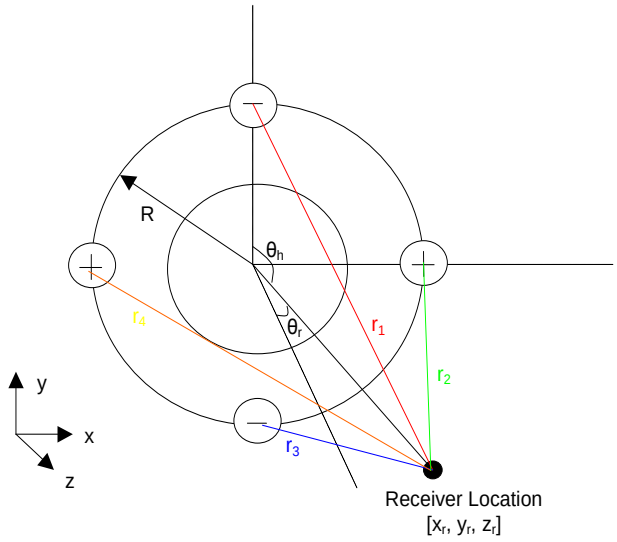

Figure 6: Mode n=2 monopole representative model

On the horizontal mid-plane, the distances between the top and bottom monopole sources, r_1 and r_3, are the same for all values of the horizontal angle θ_h and are determined as

$$r_1 = r_3 = \sqrt{r^2 + R^2}\ , \tag{1}$$

where r is the distance from the centre of the tyre to the point of observation, and R is the radius of the tyre. The distances r_2 and r_4, for the left and right monopole sources, are found using simple trigonometry (for shortness we will use a simplified notation $\theta = \theta_h$):

$$r_2 = \sqrt{(r\sin\theta - R)^2 + (r\cos\theta)^2}\,, \tag{2}$$

$$r_4 = \sqrt{(r\sin\theta + R)^2 + (r\cos\theta)^2}\,. \tag{3}$$

Similar calculations are used to determine the distances in the vertical plane (radial distances). The corresponding expressions are not shown here for brevity.

3.2 Superposition of the acoustic fields radiated by equivalent monopoles

In order to determine the level of acoustic pressure at the receiver locations a summation of the different monopole sources must be made over each mode of vibration. Using the calculated source receiver distances (see the above), the resulting radiated field can be easily calculated. For example, for the tyre vibrating on the second mode (n = 2) the resulting acoustic potential can be written as

$$\varphi_{n=2} = a_1\frac{e^{ikr_1}}{r_1} - a_2\frac{e^{ikr_2}}{r_2} + a_3\frac{e^{ikr_3}}{r_3} - a_4\frac{e^{ikr_4}}{r_4}\,. \tag{4}$$

Here the distances $r_{1\text{-}4}$ are defined by (1)-(3), and the wavenumber k for $n = 2$ is defined as $k = (2\pi f_2/c)$, where $f_2 = 132.5$ Hz is the observed resonant frequency of the second tyre mode, and $c = 343$ m/s is the sound velocity. We recall that the acoustic potential φ is related to acoustic pressure p' as $p' = -i\omega\varphi$, where $\omega = 2\pi f$ is a circular frequency. Note that in (4) the volume velocity terms are not used. Instead, the correction factors $a_{1\text{-}4}$ are used to scale the source strength between 0-1. All results are normalised and actual pressure values are not calculated. The correction factors are determined from the magnitudes of the vibrational data for each source; their values can be seen in Table 2 that shows the correction factors for all four modes of tyre vibration considered in this paper. The sources are numbered from 1 to i, clockwise with 1 being at the top position of the tyre.

Mode Number	**Correction factors**							
	a_1	**a_2**	**a_3**	**a_4**	**a_5**	**a_6**	**a_7**	**a_8**
n=1	0.67	1						
n=2	0.45	0.56	1	0.56				
n=3	0.8	0.82	0.89	1	0.89	0.82		
n=4	0.8	0.8	0.8	0.8	1	0.8	0.8	0.8

Table 2: Correction factors used for calculations of sound radiation by the first four tyre modes.

We remind the reader that the resonant frequencies of the first four tyre vibration modes are: $f_1 = 97.5$ Hz, $f_2 = 132.5$ Hz, $f_3 = 158.8$ Hz and $f_4 = 188.8$ Hz.

4 Results and discussion

In this section the results for both the experimental testing and theoretical model are analysed and compared.

4.1 Horizontal mid plane radiation patterns

Figures 7 and 8 show both the calculated radiation patterns in the mid plane position and the actual radiation patterns measured in the anechoic chamber. The normalised linear plots are in terms of acoustic pressure.

Figure 7(a) shows the theoretical radiation pattern for the n = 1 mode of vibration. For two equal monopoles with opposite phases one would expect a complete cancellation of the sound radiation in the mid plane. However, due to the scaling factors used in this work the bottom monopole has a larger source strength, which means that not a full cancellation of sound occurs. This results in radiation pattern that is constant throughout the whole range of observation angles. By comparison, Fig. 7(b) shows the radiation pattern measured experimentally for the n = 1 mode, which is significantly different from that shown in Fig. 7(a).

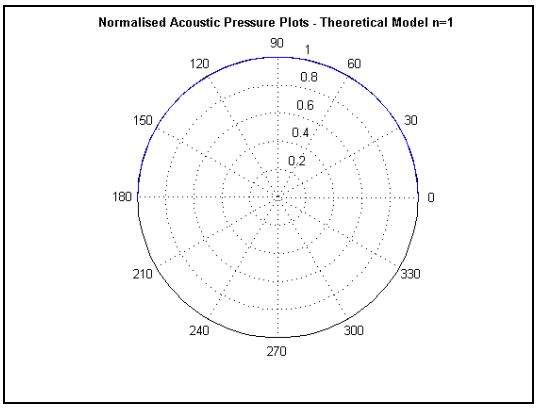

(a) n = 1

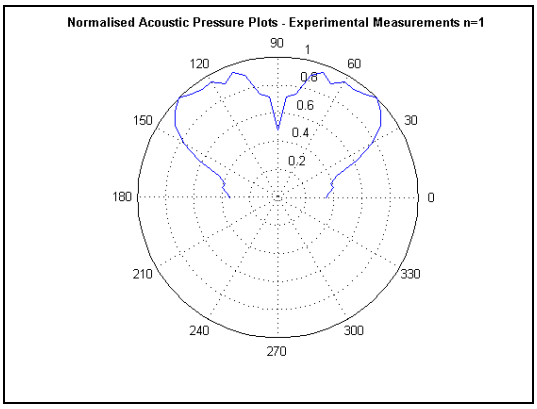

(b) n = 1

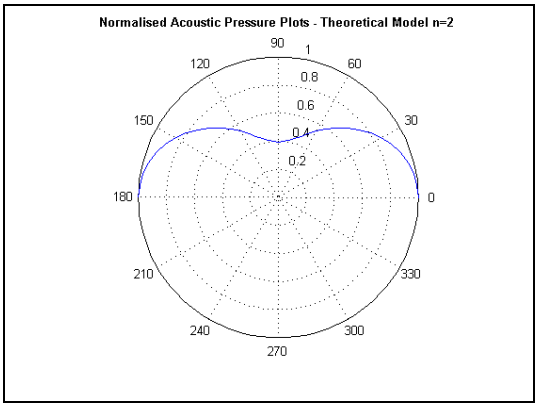

(c) n = 2

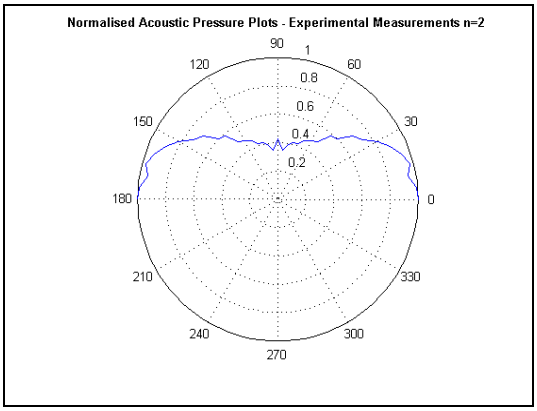

(d) n = 2

Figure 7: Calculated (a, c) and measured (b, d) sound radiation patterns in the horizontal mid plane for the tyre vibration modes n = 1 and n = 2.

Figure 7(c, d) shows the theoretical and experimental radiation patterns for the n = 2 mode. It can be seen that for this mode that the agreement between the theoretical prediction (c) and the experimental results (d) is satisfactory.

The results for n = 3 and n = 4 tyre vibration modes are given in Figure 8. As it can be seen, for these modes the agreement between the theoretical predictions (a, c) and the experimental results (b, d), although not so good as for n = 2, still can be considered as reasonable.

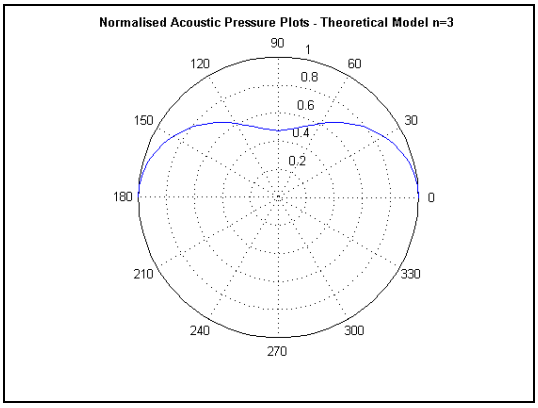

(a) n = 3

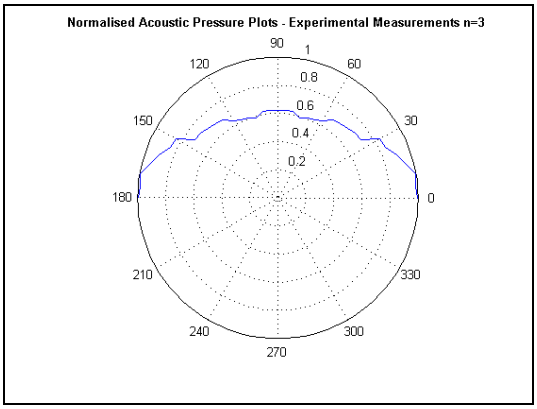

(b) n = 3

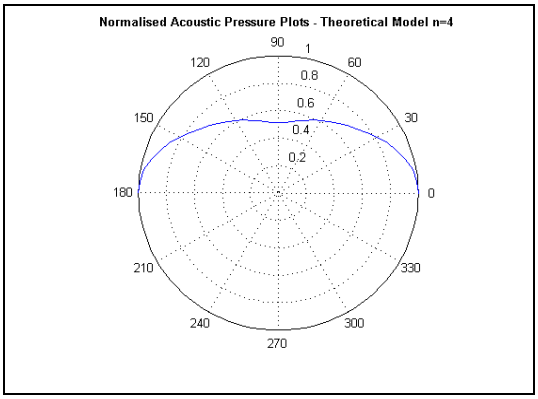

(c) n = 4

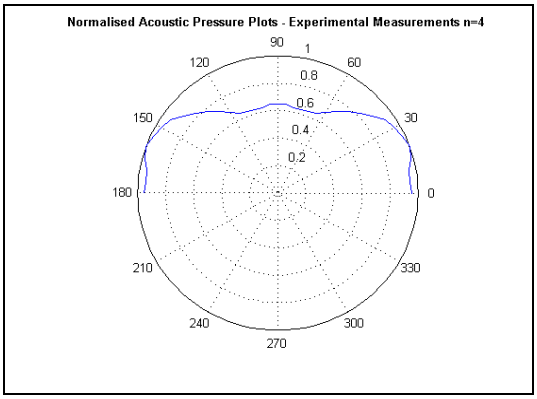

(d) n = 4

Figure 8: Calculated (a, c) and measured (b, d) sound radiation patterns in the horizontal mid plane for the tyre vibration modes n = 3 and n = 4.

4.2 Near-field acoustic measurements in the vertical plane

Figures 9 and 10 present the calculated and experimental results for the acoustic near field in the vertical plane around the circumference of the tyre. Figure 9(a) shows the theoretically calculated acoustic near-field radiated by the first mode of vibration (n = 1), using the two-monopole model. It shows the almost complete cancellation of the acoustic pressure in the mid plane which is made non zero by the scaling factor. The scaling factor also influences the maximum acoustic pressure that can be achieved at the top of the tyre shown by the smaller peak, with the maximum at the bottom monopole. By comparison, Figure 9(b) shows the result of the experimental testing for the same mode of vibration. Clearly the cancellation effect is far less significant when dealing with the actual tyre body. The acoustic pressure does fall as the mid plane is reached, but it is not as clearly defined as by the theoretical model. On the decibel scale the

difference in acoustic power is 3.5 dB from the top of the tyre to the point on the mid plane equivalent to half the maximum acoustic power intensity, so the trend is seen experimentally. Figure 9(c) shows the theoretical acoustic near-field for the second mode of tyre vibration (n = 2). It clearly shows the effect of four-monopole distribution. The amplitude of each monopole is correct with respect to the acoustic potential correction factor used. The result is almost identical to the measurements of accelerance conducted in Section 3 for this mode, thus giving some validation to the model. The model shows maxima on the horizontal and vertical mid-planes, with minima at planes 45 degrees to the maxima. The same trend is seen experimentally in Figure 9(d), with significant cancellation on the planes at 45 degrees to the maxima. Due to the fact that measurements have only been taken over a quarter of the tyre, it is not possible to see the difference in vibration amplitude between the bottom of the tyre and the top.

Strong similarities can also be seen between the model and the experimental results for the third and fourth modes of vibration, as can be seen in Figure 10(a-d). Generally, the results of the experimental testing and the theoretical modelling of near-field sound radiation in the vertical plane around the circumference of the tyre generally demonstrate a good correlation between the near field sound pressure and the corresponding mode shapes of the tyre vibration, as expected.

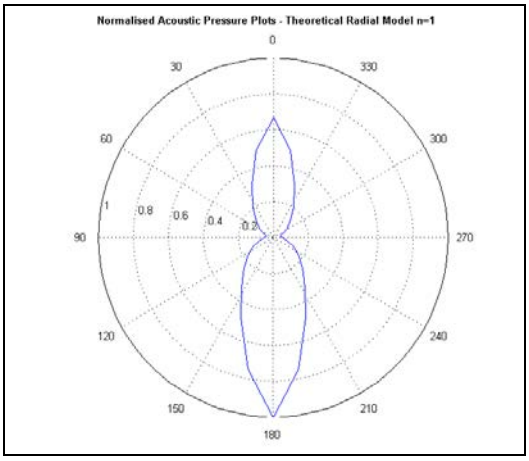

(a) n = 1

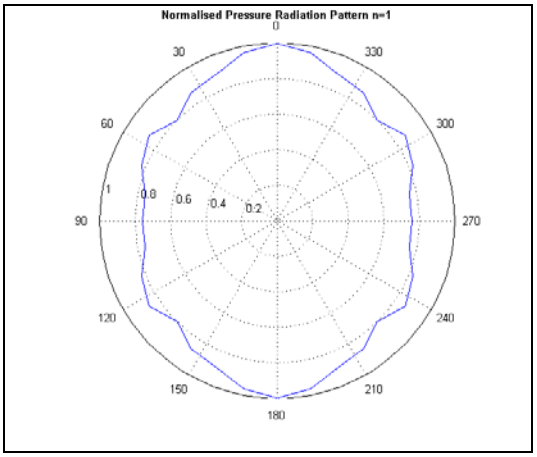

(b) n = 1

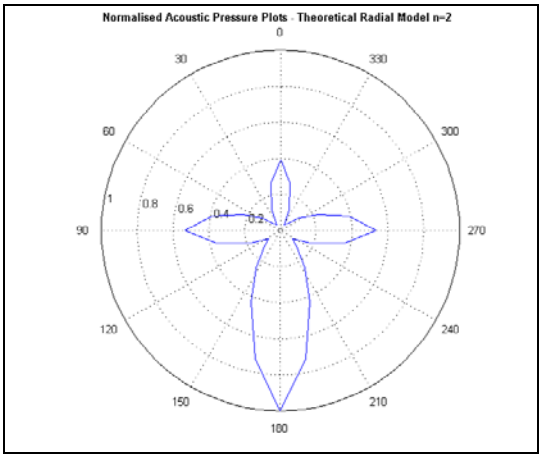

(c) n = 2

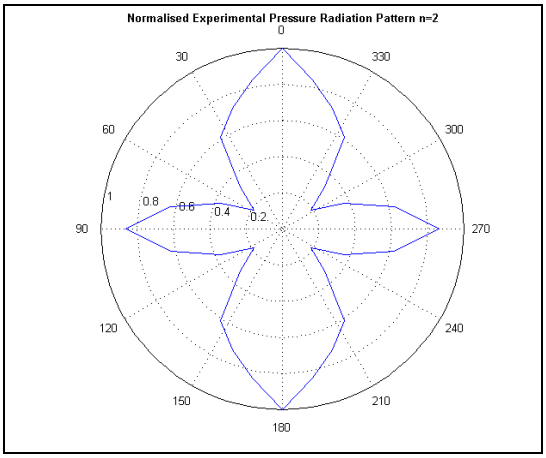

(d) n = 2

Figure 9: Calculated (a, c) and measured (b, d) acoustic near-fields in the vertical plane around the tyre circumference for the tyre vibration modes n = 1 and n = 2.

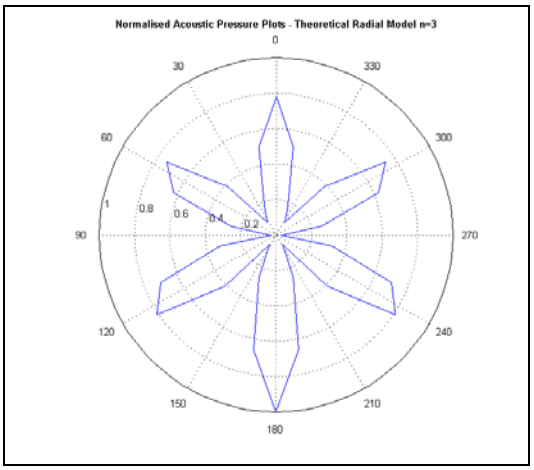

(a) n = 3

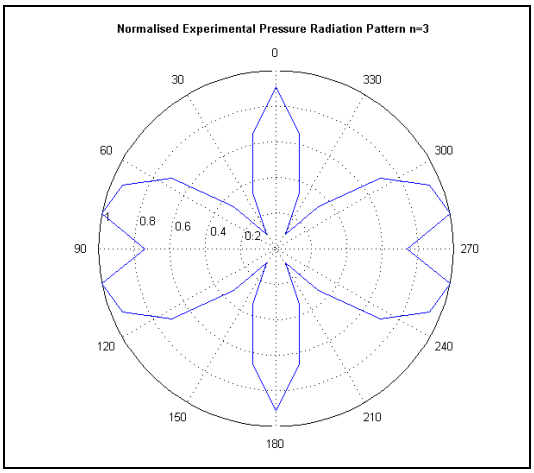

(b) n = 3

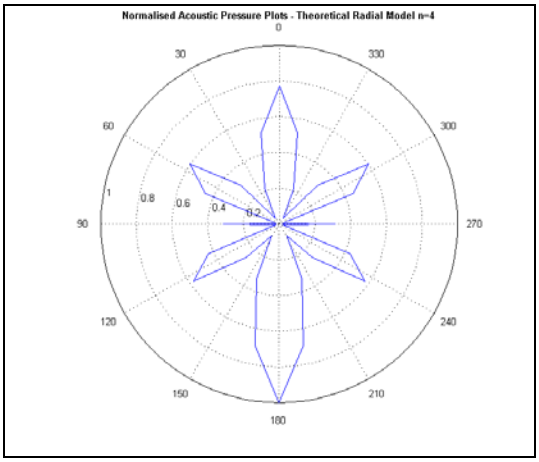

(c) n = 4

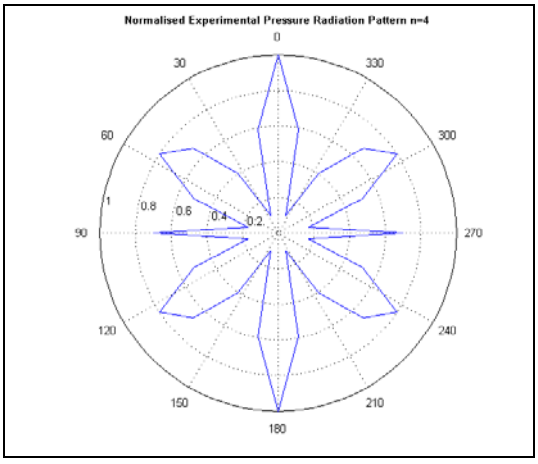

(d) n=4

Figure 10: Calculated (a, c) and measured (b, d) acoustic near-fields in the vertical plane around the tyre circumference for the tyre vibration modes n = 3 and n = 4.

5 Conclusions

It has been shown that the tyre used in this work, 155/65/R13, exhibits its modal behaviour between 90-300 Hz. Eight modes were found in this region.

The radial mode shapes of the tyre measured for the first four modes look similar to those of circular cylindrical shells. This allows the tyre to be theoretically modelled as a series of in and out of phase acoustic monopoles of varying vibration amplitude placed around the tyres circumference.

Using this simple modelling technique a reasonable level of accuracy was achieved when comparing the noise radiation patterns of the model with those measured experimentally in the anechoic chamber.

For the horizontal mid plane the trend of increasing head on noise radiation with increasing mode number matched in both cases as well as showing that maximum noise radiation occurred normal to the tread

surface. The only discrepancies were for the lowest mode at 97 Hz. The theoretical model is overly simplified for this mode to produce a distinct radiation pattern. This frequency is also below the operational frequency of the anechoic chamber, which could affect experimental results.

For the vertical near field sound radiation results, the theoretical model matched the mode shapes well with the experimental results. The sound field measurements also confirmed the vibration testing results as the areas of maximum vibration amplitude also produced maximum sound radiation in the near field. Again, accuracy increased with increasing mode number due to the increasing complexity of the model and measurement accuracy within the anechoic chamber increasing with frequency.

References

[1] M. Heckl, *Tyre noise generation*, Wear, Vol. 113, No. 1, Elsevier (1986), pp. 157–170.

[2] U. Sandberg, J.A. Ejsmont, *Tyre/Road Noise Reference Book*, Informex Ejsmont & Sandberg Handelsbolag, Harg, Kisa, Sweden (2002).

[3] B.S. Kim, G.J. Kim, T.K. Lee, *The identification of sound generating mechanisms of tyres*, Applied Acoustics, Vol. 68, No. 1, Elsevier (2007), pp. 114–133.

[4] W. Kropp, *Structure-borne sound on a smooth tyre*, Applied Acoustics, Vol. 26, No. 3, Elsevier (1989), pp. 181–192.

[5] G.J. Kim, K.R. Holland, N. Lalor, *Identification of the airborne component of tyre-induced vehicle interior noise*, Applied Acoustics, Vol. 51, No. 2, Elsevier (1997), pp. 141–156.

[6] W. Kropp, F.-X. Bécot, S. Barrelet, *On the sound radiation from tyres*, Acta Acustica united with Acustica, Vol. 86, No. 5, S. Hirzel Verlag (2000), pp. 769-779.

[7] K. Larsson, W. Kropp, *A high-frequency three-dimensional tyre model based on two coupled elastic layers*, Journal of Sound and Vibration, Vol. 253, No. 4, Elsevier (2002), pp. 889–908.

[8] J. Perisse, *A study of radial vibrations of a rolling tyre for tyre-road noise characterisation*, Mechanical Systems and Signal Processing, Vol. 16, No. 6, Elsevier (2002), pp. 1043–1058.

[9] C.-Y. Kuo, R.A.G. Graf, A.P. Dowling, W.R. Graham, *On the horn effect of a tyre/road interface, Part II: Asymptotic theories*, Journal of Sound and Vibration, Vol. 256, No. 3, Elsevier (2002), pp. 433–445.

[10] P. Jean, N. Noe, F. Gaudaire, *Calculation of tyre noise radiation with a mixed approach*, Acta Acustica united with Acustica, Vol. 94, No. 1, S. Hirzel Verlag (2008), pp. 91-103.

[11] D.J. O'Boy, A.P. Dowling, *Tyre/road interaction noise—Numerical noise prediction of a patterned tyre on a rough road surface*, Journal of Sound and Vibration, Vol. 323, No. 1-2, Elsevier (2009), pp. 270–291.

[12] P. Kindt, D. Berckmans, F. De Coninck, P. Sas, W. Desmet, *Experimental analysis of the structure-borne tyre/road noise due to road discontinuities*, Mechanical Systems and Signal Processing, Vol. 23, No. 8, Elsevier (2009), pp. 2557–2574.

[13] M.J. Gagen, *Novel acoustic sources from squeezed cavities in car tires*, Journal of the Acoustical Society of America, Vol. 106, No. 2, American Institute of Physics (1999), pp. 794-801.

[14] S. Kim, W. Jeong, Y. Park, S. Lee, *Prediction method for tire air-pumping noise using a hybrid technique*, Journal of the Acoustical Society of America, Vol. 119, No. 6, American Institute of Physics (2006), pp. 3799-3812.

[15] J. Eisenblaetter, S.J. Walsh, V.V. Krylov, *Air-related mechanisms of noise generation by solid rubber tyres with cavities*, Applied Acoustics, Vol. 71, No. 9, Elsevier (2010), pp. 854–860.

[16] K. Iwao, I. Yamazaki, *A study on the mechanism of tyre/road noise*, JSAE Review, Vol. 17, No. 2, Elsevier (1996), pp. 139-144.

[17] J.M. Cuschieri, S. Gregory, M. Tournour, *Open grid bridge noise from grid and tyre vibrations*, Journal of Sound and Vibration, Vol. 190, No. 3, Elsevier (1996), pp. 317-343.

[18] F. Fahy, *Sound and Structural Vibration: Radiation, Transmission and Response*, Academic Press, London (1985).